Monte Carlo Calculations of Electron Scattering in Photoemission*

R. N. STUART AND F. WOOTEN
Lawrence Radiation Laboratory, University of California, Livermore, California
(Received 9 November 1966)

Calculations have been made of the escape probability of a photoelectron after undergoing 0, 1, 2, ··· electron-phonon scattering events. Parameters include the mean free path for scattering by phonons, l_p, the mean free path for scattering by electrons, l_e, an optical-absorption coefficient, and a surface escape cone. Results have been tabulated so as to be of use in the analysis of photoemission data. Application of the results to experimental data on aluminum indicate $l_p \approx 130$ Å and $l_e \approx 500$ Å for electrons 9 eV above the Fermi energy.

I. INTRODUCTION

PHOTOEMISSION has attracted considerable interest in the past two or three years as a means of studying the electronic band structure of solids.[1–7] The experiments consist primarily of measurements of the energy distribution of photoelectrons emitted by monochromatic radiation, usually for a number of photon energies in the range 1.5 to 11.5 eV. Structure which is observed in the external energy distribution can then be related to structure in the density of electronic states $\rho(E)$ of the material studied. To aid in the interpretation of the energy distribution, the quantum yield (electrons emitted per photon absorbed) is also determined.

Because the electrons may undergo scattering before emission, structure in the external energy distribution may be considerably distorted compared with the initial energy distribution of the photoexcited electrons. This means that while the photoemission measurements contain information on $\rho(E)$ and various scattering mechanisms, extracting the information contained in the data can be a very difficult task when scattering plays an important role. Part of the difficulty arises simply because neither diffusion theory nor age theory is completely adequate for problems in which the source is located within a few mean free paths of the surface. However, the problem can be treated as accurately as desired by the Monte Carlo method.

In the present work, we have modified the model used earlier for the analysis of hot-electron attenuation lengths in metals.[8] We have made a number of Monte Carlo calculations for a range of scattering parameters which are of practical interest. It was not feasible to consider band structures as such. Rather, we have considered some special cases which illustrate in a quantitative way the role that scattering can play. The situation we have studied is that in which all electrons are initially excited to the same energy. The parameters which have been included are: (1) l_e, the mean free path for electron-electron (e-e) scattering; (2) l_p, the mean free path for electron-phonon (e-p) scattering; (3) an angle for the escape cone at the surface; (4) a surface scattering mechanism (specular or diffuse); and (5) a surface reflection coefficient.

Our aim has been to obtain results which, while specialized, would nonetheless be useful as an aid in the analysis of experiments. We have emphasized the role of electron-phonon scattering because it is precisely such nearly elastic scattering which is most difficult to include in a simple analytic theory. The present calculations thus serve as a check on the range of validity of analytical expressions, e.g., that of Berglund and Spicer which includes once-scattered (e-e scattering) electrons, but does not include e-p scattering.[1] As an illustrative example, we have used the present calculations to approximately determine the mean free paths for scattering in aluminum at energies 9 eV above the Fermi energy.

II. CALCULATIONS

In this section, we give a brief description of the physical model used and the assignment of parameters. A description of the essential features of the Monte Carlo program itself has been given in an earlier paper on hot electrons in metals.[8]

The parameters which must be assigned are concerned with: (1) the photoexcitation of electrons, (2) the scattering of excited electrons, and (3) the escape of photoelectrons over the surface potential barrier.

A. Optical Excitation

The optical absorption producing excited electrons is assumed to follow the usual exponential law, and an absorption coefficient α of 10^6 cm^{-1} was used. This is close to the coefficient for most metals in the visible and ultraviolet ranges. A different value of α can be used,

* Work performed under the auspices of the U. S. Atomic Energy Commission.
[1] C. N. Berglund and W. E. Spicer, Phys. Rev. **136**, A1030 (1964).
[2] C. N. Berglund and W. E. Spicer, Phys. Rev. **136**, A1044 (1964).
[3] A. J. Blodgett, Jr. and W. E. Spicer, Phys. Rev. Letters **15**, 29 (1965).
[4] A. J. Blodgett, Jr. and W. E. Spicer, Phys. Rev. **146**, 390 (1966).
[5] N. B. Kindig and W. E. Spicer, Phys. Rev. **139**, A1228 (1965).
[6] T. E. Fischer, Phys. Rev. **139**, A1228 (1965).
[7] Papers on photoemission, in *Optical Properties and Electronic Structure of Metals and Alloys*, edited by F. Abeles (North-Holland Publishing Company, Amsterdam, 1966).
[8] R. Stuart, F. Wooten, and W. E. Spicer, Phys. Rev. **135**, A495 (1964).

however, by simple scaling. An example of such scaling is given in Sec. V.

It is assumed that photoelectrons are excited in random directions. Such isotropic scattering during the excitation process has been assumed in previous analyses and seems to give reasonable agreement with experiments.[1,9] Some degree of isotropic scattering during the excitation process is to be expected for volume photoemission, and is in agreement with the work of Juenker *et al.*[10]

B. Scattering Cross Sections

Scattering events can be divided into bulk and surface scattering. The latter is included in a discussion of boundary conditions in Sec. II C. Scattering within the bulk is considered in terms of two types of scattering, inelastic and nearly elastic. Nearly elastic scattering is denoted here simply by electron-phonon scattering. Scattering by impurities, defects, and grain boundaries, all of which are nearly elastic, can be included under electron-phonon scattering.

The mean free path for scattering by phonons, l_p, was taken as an adjustable parameter. It is, in fact, the parameter of greatest interest here. To determine how many electrons escaped after having undergone 0, 1, 2, 3, $\cdots$ scatterings by phonons, a small energy loss was assigned to each such collision. Then, by keeping account of the energy of each electron, it was easily determined how many e-p scattering events each photoelectron had suffered. Note that, in the present case, the assignment of an energy loss is purely a convenient bookkeeping scheme.

Inelastic collisions consist of electron-electron scattering and, for electrons with sufficient energy, electron-plasmon excitation. Both processes can be included under e-e scattering here, since we are concerned only with the mean free path for inelastic scattering of electrons of a single initial energy and not with what happens after they have suffered a large energy loss.

Electron-electron scattering is assumed to be such that all possible transitions are equally probable. That is, the transitions are taken to be dependent upon the product of initial and final densities of states for all energy-conserving transitions. In such a case, the probability that an electron with energy E will be scattered to an energy between E' and $(E'+dE')$ is

$$P(E',E)dE' = k\left\{\int_{E_f-(E-E')}^{E_f} \rho(E'')\rho[E''+(E-E')]dE''\right\} \times\rho(E')dE'. \quad (1)$$

[9] F. Wooten, T. Huen, and R. N. Stuart, in *Optical Properties and Electronic Structure of Metals and Alloys*, edited by F. Abeles (North-Holland Publishing Company, Amsterdam, 1966), p. 333.
[10] D. W. Juenker, J. P. Waldron, and R. J. Jaccodine, J. Opt. Soc. Am. 54, 216 (1964).

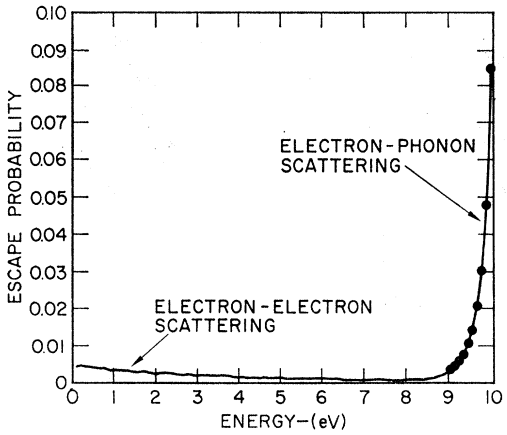

FIG. 1. Separation of electron-electron scattering from electron-phonon scattering for $l_e=600$ Å, $l_p=100$ Å and an escape cone of 2π sr. Most of the inelastically scattered electrons have been scattered to below the vacuum level ($E=0$). An energy loss of 0.1 eV was assigned to each e-p scattering event.

The integration over E'' is such as to include all possible energy-conserving secondary excitations of electrons from below the Fermi energy E_f. The probability that an electron with energy E will be scattered to some other energy is then

$$P(E)=\int_{E_f}^{E} P(E,E')dE'. \quad (2)$$

With appropriate units having been chosen for the density of states, the constant k in Eq. (1) is then a parameter which determines the cross section for e-e scattering.

In the present calculation, the initial energy of the excited electrons was chosen such that $E-E_f \gg E$ (phonon). That is, the total range of energy losses available was such that e-p scattering could be unambiguously distinguished from e-e scattering. This is illustrated graphically in Fig. 1.

Since the concern here is with scattering of an electron from a particular energy interval and not with the energy after scattering, a constant density of states was assumed for convenience. The constant k in Eq. (1) was then chosen to give the desired cross section, or mean free path l_e, for e-e scattering.

C. Boundary Conditions

During the course of its random motion through a crystal, an electron may reach the vacuum surface. If its normal component of momentum corresponds to an energy greater than the surface-barrier height, it is counted as an escaping electron, and its external kinetic energy is recorded. From 50 000 to 250 000, such calculations were made for each set of parameters. The data were then printed in tabular form and also presented graphically, as in Fig. 1.

TABLE I. Escape probability for an escape cone of 2π sr. The mean free path for electron-electron scattering is denoted by l_e and for electron-phonon scattering by l_p. The number of electron-phonon scattering events before escape is denoted by an integer n. The escape probability is given for each value of n. The total escape probability for electrons escaping after only undergoing nearly elastic collisions is given in the row labeled $\sum_n$.

l_p (Å)	40	100	250	600	1000
			$l_e=15$ Å		
$n=0$	0.0254	0.0304	0.0336	0.033	0.0357
1	0.0051	0.0029	0.0014	0.0005	0.0003
2	0.0013	0.0003			
3	0.0003				
4	0.0002				
$\sum_n$	0.0323	0.0336	0.0350	0.0335	0.0360
			$l_e=40$ Å		
$n=0$	0.0442	0.0602	0.0712	0.0771	0.0779
1	0.0160	0.0123	0.0070	0.0032	0.0019
2	0.0064	0.0027	0.0006		
3	0.0030	0.0006			
4	0.0013				
5–9	0.0008				
$\sum_n$	0.0717	0.0758	0.0788	0.0803	0.0798
			$l_e=100$ Å		
$n=0$	0.0616	0.0950	0.1224	0.1390	0.1459
1	0.0322	0.0336	0.0237	0.0138	0.0090
2	0.0187	0.0128	0.0051	0.0014	0.0003
3	0.0114	0.0050	0.0010		
4	0.0062	0.0024	0.0003		
5–9	0.0107	0.0013			
10–19	0.0011				
$\sum_n$	0.1419	0.1501	0.1525	0.1542	0.1552
			$l_e=250$ Å		
$n=0$	0.0718	0.1195	0.1742	0.2107	0.2243
1	0.0442	0.0592	0.0539	0.0360	0.0250
2	0.0290	0.0312	0.0182	0.0066	0.0030
3	0.0216	0.0181	0.0066	0.0018	0.0006
4	0.0162	0.0104	0.0029		
5–9	0.0381	0.0154	0.0018		
10–19	0.0149	0.0016			
10–29	0.0024				
$\sum_n$	0.2382	0.2554	0.2576	0.2551	0.2529
			$l_e=600$ Å		
$n=0$	0.0749	0.1371	0.2070	0.2690	0.2923
1	0.0507	0.0778	0.0848	0.0690	0.0533
2	0.0366	0.0479	0.0410	0.0216	0.0117
3	0.0283	0.0325	0.0205	0.0070	0.0027
4	0.0232	0.0224	0.0117	0.0027	0.0006
5–9	0.0669	0.0480	0.0103	0.0014	
10–19	0.0466	0.0157	0.0165		
20–29	0.0138	0.0014			
≥ 30	0.0085				
$\sum_n$	0.3263	0.3828	0.3918	0.3707	0.3606
			$l_e=1000$ Å		
$n=0$	0.0768	0.1451	0.2216	0.2928	0.3208
1	0.0528	0.0842	0.0998	0.0894	0.0722
2	0.0392	0.0549	0.0518	0.0325	0.0206
3	0.0310	0.0394	0.0314	0.0133	0.0074
4	0.0258	0.0285	0.0174	0.0067	0.0022
5–9	0.0810	0.0666	0.0301	0.0054	0.0013
10–19	0.0682	0.0320	0.0037		
20–29	0.0259	0.0061			
≥ 30	0.0232	0.0022			
$\sum_n$	0.4239	0.4590	0.4558	0.4401	0.4245

All calculations were made with a convenient set of energy parameters; that is, a convenient choice of E, E_f, band minimum, and work function. Rather than presenting results in terms of energy, however, we have calculated the solid angle of the escape cone for the particular set of energy parameters used. The results are thus tabulated here in a more generally useful form.

Should the electron not have enough momentum to escape, it is scattered back into the crystal. It is assumed that no energy loss is associated with surface scattering. Nearly all calculations have been made for specular surface scattering, that is, for scattering in which the angles of incidence and reflection are equal. A few calculations were made for diffuse scattering in which the reflected electrons follow Lambert's law. The calculations show, as will be seen later, that the kind of surface scattering does not really matter.

A few calculations were made with a surface-transmission coefficient less than unity. These cases are labeled as such. Otherwise, all results are for a transmission coefficient of unity, as implied above.

III. RESULTS

Table I gives the escape probability for an escape cone of 2π sr. Since, for that escape cone, all electrons which arrive at the surface also escape, Table I gives also the probability of arrival at the surface.

Tables II–IV give the escape probability for escape cones of 1.18π, 0.586π, and 0.211π sr. Note that, because the probability of escape is biased in favor of those electrons which are headed perpendicular to the surface, the escape probability is not proportional to the solid angle of the escape cone.

Specular surface scattering has been used for Tables I–IV (clearly irrelevant for Table I, but not necessarily *a priori* so for Tables II–IV).

Table V gives the escape probability for an escape cone of 0.586π sr, a transmission coefficient of 0.5, and specular surface scattering. The intent was to study a situation in which $l_p \ll l_e$, so that the effect of phonon scattering on electrons reflected by a quantum-mechanical reflection coefficient could be studied. As expected, the number of electrons escaping after only a few phonon scatterings is cut in half (compare with column 1 of Table III). Over all, because of an enhancement from *e-p* scattering, the yield is not reduced by 50%. For those more likely situations, however, in which $l_p \gtrsim l_e$, the effect of a transmission coefficient is simply to multiply the yield (calculated without a transmission coefficient) by the transmission coefficient.

Table VI was calculated for the same set of parameters as Table V, except for the fact that diffuse surface scattering was used. It is clear that the type of surface scattering has no significant effect on the escape probability.

TABLE II. Escape probability for an escape cone of 1.18π sr. The mean free path for electron-electron scattering is denoted by l_e and for electron-phonon scattering by l_p. The number of electron-phonon scattering events before escape is denoted by an integer n. The escape probability is given for each value of n. The total escape probability for electrons escaping after only undergoing nearly elastic collisions is given in the row labeled $\sum_n$.

l_p (Å)	40	100	250	600	1000
		$l_e=15$ Å			
$n=0$	0.0211	0.0248	0.0267	0.0269	0.0274
1	0.0046	0.0026	0.0011	0.0005	0.0002
2	0.0012	0.0003	0.0002		
3	0.0003				
$\sum_n$	0.0272	0.0277	0.0280	0.0274	0.0276
		$l_e=40$ Å			
$n=0$	0.0355	0.0477	0.0566	0.0605	0.0618
1	0.0152	0.0109	0.0061	0.0029	0.0018
2	0.0064	0.0026	0.0006		
3	0.0026	0.0006	0.0002		
4	0.0013	0.0002			
5–9	0.0008				
$\sum_n$	0.0618	0.0620	0.0635	0.0634	0.0636
		$l_e=100$ Å			
$n=0$	0.0491	0.0762	0.0978	0.1098	0.1149
1	0.0288	0.0302	0.0211	0.0110	0.0075
2	0.0174	0.0122	0.0046	0.0014	0.0005
3	0.0106	0.0051	0.0011	0.0003	
4	0.0066	0.0024	0.0003		
5–9	0.0099	0.0014			
10–19	0.0011				
$\sum_n$	0.1235	0.1275	0.1249	0.1225	0.1229
		$l_e=250$ Å			
$n=0$	0.0554	0.0973	0.1357	0.1619	0.1706
1	0.0389	0.0518	0.0477	0.0310	0.0222
2	0.0267	0.0294	0.0179	0.0064	0.0032
3	0.0202	0.0171	0.0069	0.0014	0.0006
4	0.0146	0.0102	0.0024	0.0003	
5–9	0.0342	0.0147	0.0016		
10–19	0.0117	0.0018			
$\sum_n$	0.2017	0.2223	0.2122	0.2010	0.1966
		$l_e=600$ Å			
$n=0$	0.0578	0.1077	0.1605	0.1986	0.2117
1	0.0443	0.0691	0.0760	0.0616	0.0469
2	0.0328	0.0454	0.0387	0.0206	0.0115
3	0.0264	0.0314	0.0203	0.0074	0.0032
4	0.0203	0.0219	0.0115	0.0029	0.0008
5–9	0.0610	0.0480	0.0142	0.0015	
10–19	0.0323	0.0074	0.0010		
$\sum_n$	0.2749	0.3309	0.3222	0.2926	0.2741
		$l_e=1000$ Å			
$n=0$	0.0610	0.1123	0.1698	0.2107	0.2268
1	0.0470	0.0750	0.0886	0.0797	0.0659
2	0.0371	0.0523	0.0493	0.0315	0.0214
3	0.0304	0.0378	0.0299	0.0149	0.0058
4	0.0251	0.0291	0.0181	0.0072	0.0026
5–9	0.0819	0.0699	0.0296	0.0072	0.0015
10–19	0.0682	0.0342	0.0042		
20–29	0.0277	0.0066			
≥30	0.0253	0.0013			
$\sum_n$	0.4037	0.4185	0.3895	0.3512	0.3241

IV. DISCUSSION

Scattering by phonons sometimes plays an important role, and it is a role that is easily overlooked. One of the main effects is to increase the average total path traveled by an electron for a particular net displacement. Electron-phonon scattering thus increases the probability of e-e scattering for a particular net displacement, and may result in a reduced quantum yield. It may also increase the quantum yield by increasing the escape probability. This can happen because an electron which reaches the surface and does not escape, but is reflected from the surface back into the solid, may then be redirected towards the surface by later scattering events and thus have several more chances to escape. Which of the effects dominates depends on the relative values of α^{-1}, l_e, and l_p, as well as the escape cone.

If $l_p \gtrsim l_e$, and the escape cone is large (Tables I and II), e-p scattering need not be considered. Even though some electrons escape after having undergone several e-p scattering events, the total escape probability remains essentially constant for electrons escaping with no appreciable energy loss. Only when l_p is less than the mean optical-absorption depth α^{-1} is there a decrease in the quantum yield. The latter is an example of a decrease in yield arising from increased e-e scattering which, in turn, is brought about by increased e-p scattering. Electrons excited at depths greater than l_p below the surface then have significantly less chance of reaching the surface.

The calculations show that, for high-energy electrons, where the total escape probability is almost constant for all values of $l_p \gtrsim l_e$ and α^{-1}, one should not expect any appreciable change in photoemission with temperature. This is generally found to be true experimentally. A lower temperature might sharpen up structure slightly by decreasing the amount of e-p scattering, but no significant temperature dependence of the fundamental optical excitation is likely when well above the absorption threshold.[11]

A first conclusion is that analytical approximations need not include scattering by phonons whenever the escape cone is large and $l_p \gtrsim l_e$ and α^{-1}. Since the latter condition probably holds in most metals for electrons more than a few eV above the Fermi energy, the validity of analytical expressions may often be quite good for electrons emitted at very high energies, i.e., the high-energy tail of the energy distribution when $h\nu$ is large.

For electrons emitted at low energies or, more correctly, with a small escape cone, a great deal of care is required. This is the region which is most difficult to study. Here, the photoelectrons may include many electrons not optically excited to the low-energy region, but scattered there from higher energies. The whole situation may then be further complicated by a very significant effect from phonon scattering. Tables III

[11] An important exception may arise when the optical properties are affected by a coupling of transverse electromagnetic waves to longitudinal plasmons via phonons. See, e.g., J. J. Hopfield, Phys. Rev. 139, A419 (1965).

TABLE III. Escape probability for an escape cone of 0.586π sr. The mean free path for electron-electron scattering is denoted by l_e and for electron-phonon scattering by l_p. The number of electron-phonon scattering events before escape is denoted by an integer n. The escape probability is given for each value of n. The total escape probability for electrons escaping after only undergoing nearly elastic collisions is given in the row labeled $\sum_n$.

l_p (Å)	40	100	250	600	1000
		$l_e=15$ Å			
$n=0$	0.0120	0.0144	0.0155	0.0162	0.0157
1	0.0030	0.0018	0.0008	0.0002	0.0002
2	0.0008	0.0003			
3	0.0002				
4	0.0002				
$\sum_n$	0.0162	0.0165	0.0163	0.0164	0.0159
		$l_e=40$ Å			
$n=0$	0.0203	0.0272	0.0323	0.0347	0.0346
1	0.0094	0.0074	0.0037	0.0019	0.0011
2	0.0042	0.0018	0.0005		0.0002
3	0.0021	0.0005	0.0002		
4	0.0010	0.0002			
5–9	0.0008				
$\sum_n$	0.0378	0.0371	0.0367	0.0366	0.0359
		$l_e=100$ Å			
$n=0$	0.0280	0.0430	0.0549	0.0622	0.0642
1	0.0182	0.0187	0.0130	0.0069	0.0048
2	0.0112	0.0082	0.0034	0.0010	0.0003
3	0.0074	0.0038	0.0008	0.0002	
4	0.0051	0.0018	0.0003		
5–9	0.0085	0.0016	0.0002		
10–19	0.0010				
$\sum_n$	0.0371	0.0771	0.0726	0.0703	0.0693
		$l_e=250$ Å			
$n=0$	0.0302	0.0549	0.0762	0.0880	0.0914
1	0.0250	0.0328	0.0293	0.0192	0.0138
2	0.0184	0.0198	0.0118	0.0045	0.0019
3	0.0147	0.0123	0.0050	0.0006	0.0003
4	0.0117	0.0077	0.0022	0.0002	
5–9	0.0317	0.0115	0.0016	0.0002	
10–19	0.0149	0.0014			
20–29	0.0022				
≥ 30	0.0002				
$\sum_n$	0.1490	0.1404	0.1261	0.1127	0.1074
		$l_e=600$ Å			
$n=0$	0.342	0.614	0.1008	0.1256	0.1107
1	0.0280	0.434	0.0458	0.0376	0.0286
2	0.0237	0.0307	0.0259	0.0141	0.0085
3	0.0197	0.0226	0.0154	0.0061	0.0024
4	0.0163	0.0170	0.0086	0.0024	0.0008
5–9	0.0544	0.0406	0.0133	0.0019	0.0003
10–19	0.0446	0.0160	0.0010		
20–29	0.0155	0.0024			
≥ 30	0.0115	0.0003			
$\sum_n$	0.2479	0.2344	0.2108	0.1877	0.1513
		$l_e=1000$ Å			
$n=0$	0.0349	0.0627	0.0914	0.1114	0.1179
1	0.0302	0.0467	0.0541	0.0478	0.0406
2	0.0259	0.0355	0.0344	0.0230	0.0147
3	0.0224	0.0275	0.0227	0.0114	0.0056
4	0.0189	0.0218	0.0146	0.0056	0.0026
5–9	0.0656	0.0594	0.0288	0.0070	0.0021
10–19	0.0637	0.0341	0.0054	0.0006	
20–29	0.0286	0.0078			
≥ 30	0.0301	0.0027			
$\sum_n$	0.3203	0.2982	0.2514	0.2068	0.1835

and IV show that e-p scattering cannot be ignored at low energy.

The increase in total escape probability at low energy due to e-p scattering is easy to understand. If an electron has energy only slightly in excess of that required for emission, it must be headed almost perpendicular to the surface in order to escape. Otherwise, the electron will be reflected back into the solid. Now, as mentioned earlier, the electron may have several chances to escape before it suffers an e-e scattering event, especially if $l_p<l_e$. Furthermore, it is just at low energies that the ratio l_p/l_e is smallest.

It is clear that it is generally necessary to consider e-p scattering in the analysis of low-energy photoemission data. A method of procedure valid in some cases is to first analyze the high-energy tail of the photoelectron distribution with the help of Tables I–IV. The main difficulty is in estimating the escape cone when treating the excited electrons as a free-electron gas. When the method is feasible, a value of l_e can be determined for the high-energy electrons.[12] Then, assuming that the density of states is known, one can calculate $l_e(E)$ from Eq. (2), after having chosen k from Eq. (1) to give agreement with the known l_e.

To determine the complete energy distribution and the contribution of scattered electrons, an analytical approximation can be used. Perhaps the most appropriate is that of Berglund and Spicer.[1] It does not include e-p scattering explicitly. Nonetheless, particularly as used by Blodgett and Spicer,[4] it accounts for such scattering, to a large extent, by an escape function $T(E)$, which is determined empirically from the data. Tables I–IV can then be of help in determining the self-consistency of the solution.

V. APPLICATION TO ALUMINUM

The external energy distribution and quantum yield has been measured for aluminum in the vacuum ultraviolet range.[9] From this information, the differential quantum yield (electrons per photon per eV) can be calculated. With monochromatic light of energy 9.18 eV, the differential quantum yield for electrons excited from just below the Fermi level to nearly 5 eV above the vacuum level (the work function is 4.2 eV) is approximately 0.014. To determine the escape probability for these electrons, we now need to calculate the density in energy (electrons per eV) of electrons excited from just below the Fermi level per absorbed photon.

The total number of transitions possible is given by a product of initial and final densities of states integrated over the range of possible transitions. For aluminum,

[12] One of the virtues of photoemission experiments is that they can often be used to determine scattering cross sections in an energy range not generally accessible by other means. Berglund and Spicer (Ref. 2) estimated l_e in Cu from lifetime broadening effects in the photoelectron energy distribution. Obtaining l_e directly from the yield and Tables I–IV is a more sensitive method when feasible.

TABLE IV. Escape probability for an escape cone of 0.211π sr. The mean free path for electron-electron scattering is denoted by l_e and for electron-phonon scattering by l_p. The number of electron-phonon scattering events before escape is denoted by an integer n. The escape probability is given for each value of n. The total escape probability for electrons escaping after only undergoing nearly elastic collisions is given in the row labeled $\sum_n$.

l_p (Å)	40	100	250	600	1000
		$l_e=15$ Å			
$n=0$	0.0053	0.0063	0.0065	0.0068	0.0063
1	0.0014	0.0008	0.0005	0.0002	
2	0.0004	0.0001			
3	0.0001				
$\sum_n$	0.0072	0.0072	0.0070	0.0070	0.0063
		$l_e=40$ Å			
$n=0$	0.0085	0.0114	0.0129	0.0144	0.0140
1	0.0042	0.0033	0.0018	0.0011	0.0006
2	0.0020	0.0008	0.0002		
3	0.0010	0.0002			
4	0.0004				
5–9	0.0003				
$\sum_n$	0.0164	0.0157	0.0149	0.0155	0.0146
		$l_e=100$ Å			
$n=0$	0.0109	0.0168	0.0204	0.0240	0.0250
1	0.0077	0.0077	0.0057	0.0029	0.0020
2	0.0052	0.0038	0.0014	0.0003	0.0001
3	0.0033	0.0016	0.0004	0.0001	
4	0.0023	0.0007	0.0002		
5–9	0.0041	0.0005			
10–19	0.0008				
$\sum_n$	0.0342	0.0315	0.0281	0.0273	0.0271
		$l_e=250$ Å			
$n=0$	0.0122	0.0212	0.0278	0.0327	0.0350
1	0.0108	0.0138	0.0126	0.0083	0.0055
2	0.0087	0.0089	0.0056	0.0022	0.0010
3	0.0072	0.0056	0.0024	0.0005	0.0002
4	0.0057	0.0035	0.0012	0.0001	0.0001
5–9	0.0159	0.0058		0.0001	
10–19	0.0089	0.0011			
20–29	0.0016				
≥ 30	0.0006				
$\sum_n$	0.0713	0.0599	0.0506	0.0439	0.0418
		$l_e=600$ Å			
$n=0$	0.0126	0.0224	0.0329	0.0393	0.0429
1	0.0124	0.0180	0.0202	0.0162	0.0121
2	0.0102	0.0137	0.0122	0.0068	0.0037
3	0.0088	0.0110	0.0070	0.0028	0.0013
4	0.0081	0.0085	0.0044	0.0015	0.0005
5–9	0.0284	0.0235	0.0077	0.0013	0.0004
10–19	0.0285	0.0117	0.0011		
20–29	0.0117	0.0018			
≥ 30	0.0211	0.0004			
$\sum_n$	0.1418	0.1110	0.0855	0.0679	0.0609
		$l_e=1000$ Å			
$n=0$	0.0134	0.0236	0.0337	0.0424	0.0434
1	0.0124	0.0194	0.0227	0.0199	0.0168
2	0.0112	0.0157	0.0153	0.0103	0.0067
3	0.0103	0.0120	0.0100	0.0053	0.0027
4	0.0098	0.0105	0.0072	0.0030	0.0014
5–9	0.0352	0.0318	0.0156	0.0034	0.0010
10–19	0.0403	0.0219	0.0043	0.0003	
20–29	0.0208	0.0054	0.0003		
≥ 30	0.0170	0.0023			
$\sum_n$	0.1704	0.1426	0.1091	0.0846	0.0720

TABLE V. Escape probability for an escape cone of 0.586π sr, a transmission coefficient of 0.5, and specular surface scattering. The mean free path for electron-electron scattering is 1000 Å and for electron-phonon scattering 40 Å. The number of electron-phonon scattering events before escape is denoted by an integer n. The escape probability is given for each value of n. The total escape probability for electrons escaping after only undergoing nearly elastic collisions is given in the row labeled $\sum_n$.

$l_e=1000$ Å, $l_p=40$ Å	
$n=0$	0.0178
1	0.0155
2	0.0138
3	0.0115
4	0.0104
5–9	0.0392
10–19	0.0440
20–29	0.0213
≥ 30	0.0278
$\sum_n$	0.2013

which is a nearly free-electron gas metal, the density of states is given approximately by $\rho(E)=CE^{1/2}$. Thus, the total number of energy-conserving transitions is

$$N=C^2\int_{E_f-h\nu}^{E_f} E^{1/2}(E+h\nu)^{1/2}dE. \tag{3}$$

The density of excitations from the Fermi energy, $n(E_f)$, is then

$$n(E_f)=\rho(E_f)\rho(E_f+h\nu)/N, \tag{4}$$

provided all transitions are equally probable. The latter requirement seems to be satisfied quite well in a large number of cases.[1–5,9]

Evaluating Eqs. (3) and (4) with $E_f=11.7$ eV and $h\nu=9.18$ eV yields

$$n(E_f)=0.123 \text{ electrons per photon per eV.}$$

Thus, the escape probability for electrons excited to 5 eV above the vacuum level is $0.014/0.123=0.114$.

TABLE VI. Escape probability for an escape cone of 0.586π sr, a transmission coefficient of 0.5, and diffuse surface scattering. The mean free path for electron-electron scattering is 1000 Å and for electron-phonon scattering 40 Å. The number of electron-phonon scattering events before escape is denoted by an integer n. The escape probability is given for each value of n. The total escape probability for electrons escaping after only undergoing nearly elastic collisions is given in the row labeled $\sum_n$.

$l_e=1000$ Å, $l_p=40$ Å	
$n=0$	0.0170
1	0.0157
2	0.0139
3	0.0122
4	0.0106
5–9	0.0416
10–19	0.0461
20–29	0.0226
≥ 30	0.0280
$\sum_n$	0.2077

The minimum energy necessary for escape is $E_f+e\phi$ or, in aluminum, 15.9 eV. Electrons excited from near the Fermi energy by absorpton of photons with $h\nu=9.18$ eV have an energy of nearly 20.9 eV. The escape cone for these electrons is easily determined and is found to be approximately 0.26π.

The escape cone for Table IV is not much less than 0.26π. By interpolating between Tables III and IV, it is seen that the escape probability is tatisfied by mean free paths between $l_p=100$ Å, $l_e=600$ Å and $l_p=250$ Å, $l_e=1000$ Å. Because α^{-1} for aluminum is 67 Å while the tables were constructed for $\alpha^{-1}=100$ Å, it is necessary to scale the results. Thus, for electrons in aluminum, which are about 9 eV above the Fermi energy, the mean free paths are between $l_p=67$ Å, $l_e=400$ Å and $l_p=167$ Å, $l_e=667$ Å. This just spans the values $l_p=130$ Å, $l_e=510$ Å which were found to give the best fit when a detailed analysis was made of the entire energy distribution of electrons emitted from aluminum.[9] It should be noted, though, that Quinn's theoretical calculation of l_e in aluminum[13] indicates a value of about 50 Å for electrons of energy greater than 5 eV above the Fermi energy, and appears to be in substantial disagreement with our analysis of the experimental results.

[13] J. J. Quinn, Phys. Rev. **126**, 1453 (1962).

PHYSICAL REVIEW VOLUME 156, NUMBER 2 10 APRIL 1967

Properties of the Mn^{55} Nuclear-Magnetic-Resonance Modes in $CsMnF_3$†

L. B. WELSH*
Department of Physics, University of California, Berkeley, California
(Received 20 June 1966)

A new NMR mode of the Mn^{55} nuclei in the hexagonal antiferromagnet $CsMnF_3$ has been observed directly between 673 and 676 Mc/sec. This mode results from the difference in the hyperfine couplings for nuclei of the Mn1 and Mn2 sites when the nuclei are strongly coupled by the Suhl-Nakamura (SN) interaction. The new NMR mode resembles an antiferromagnetic (AFM) exchange mode, while the NMR mode observed by Minkiewicz resembles an acoustic AFM mode. The linewidths of the acoustic and exchange NMR modes at 5000 Oe are 0.042 and 0.22 Mc/sec, respectively. These are a factor of ten narrower than predicted from the SN interaction. A four-sublattice model of $CsMnF_3$ is proposed which accounts for the field dependence of both NMR modes. The NMR frequencies extrapolated to infinite nuclear temperature are 666.0 ± 0.2 Mc/sec for the Mn2 site and 676.85 ± 0.1 Mc/sec for the Mn1 site. This suggests zero-point spin-wave reductions of $(2.2\pm1.0)\%$ and $(3.2\pm1.0)\%$ for the Mn1 and Mn2 sites; Davis's calculation predicts 2.49% and 4.36%, respectively. The temperature dependence of the electron-sublattice magnetization is determined from the temperature dependence of the exchange NMR mode. Four-sublattice-model spin-wave calculations account for this temperature dependence when an intrasublattice ferromagnetic exchange energy is included which is 32% of the antiferromagnetic intersublattice exchange energy. The Mn^{55} nuclear spin-lattice relaxation times have been determined for fields between 600 and 5000 Oe and for temperatures between 1.4 and 4.2°K. The field dependence and magnitude of the relaxation times are not understood, but at 5000 Oe, $T_1\propto T^{-4.96\pm0.03}$ with T_1 equal to 3.7 sec at 1.4°K. This temperature dependence indicates that three-magnon processes may be responsible for the relaxation.

I. INTRODUCTION

THE magnetic properties of the hexagonal antiferromagnet $CsMnF_3$ have been the subject of several previous studies. Torsion measurements, susceptibility measurements, antiferromagnetic resonance (AFR) studies, and electron-nuclear double-resonance studies have been performed by Lee *et al.*[1] Witt and Portis used the method of electron-nuclear double resonance to measure the Mn^{55} nuclear spin-lattice relaxation time[2] and to investigate the diffusion of energy in the nuclear spin system.[3] Minkiewicz and Nakamura[4] studied the Mn^{55} nuclear magnetic resonance (NMR) directly.

In Sec. II we discuss the direct observation of a second Mn^{55} nuclear resonance mode in $CsMnF_3$. A four-sublattice model for $CsMnF_3$ is described which accounts for the observed behavior of both NMR modes. For the two inequivalent Mn^{2+} sites the hyperfine coupling constants and the zero-point spin reductions are determined and compared with theory. From

† Supported by the U. S. Atomic Energy Commission through Contract AT(11-1)-34 Project 47. Report Code UCB-34P47-2.
* Present address: Department of Physics, University of Pennsylvania, Philadelphia, Pennsylvania.
[1] K. Lee, A. M. Portis, and G. L. Witt, Phys. Rev. **132**, 144 (1963).
[2] G. L. Witt and A. M. Portis, Phys. Rev. **136**, A136 (1964).
[3] G. L. Witt, thesis, University of California, 1964 (unpublished).
[4] V. Minkiewicz and A. Nakamura, Phys. Rev. **143**, 361 (1966).